British Journal of Pharmacology (1999) 127, 243–251
http://www.stockton-press.co.uk/bjp

Inhibition of HERG channels stably expressed in a mammalian cell line by the antianginal agent perhexiline maleate

*,[1,3]B.D. Walker, [2]S.M. Valenzuela, [1]C.B. Singleton, [1]H. Tie, [1]J.A. Bursill, [1]K.R. Wyse, [2]M.R. Qiu, [2]S.N. Breit & [1]T.J. Campbell

[1]Department of Clinical Pharmacology, University of New South Wales, Victor Chang Cardiac Research Institute, St Vincent's Hospital, Darlinghurst NSW 2010, Australia and [2]Centre for Immunology, St Vincent's Hospital, Sydney, NSW 2010, Australia and [3]Department of Medicine, St Vincent's Hospital, Darlinghurst, NSW 2010, Australia

1 Perhexiline has been used as an anti-anginal agent for over 25 years, and is known to cause QT prolongation and *torsades de pointes*. We hypothesized that the cellular basis for these effects was blockade of I_{Kr}.

2 A stable transfection of HERG into a CHO-K1 cell line produced a delayed rectifier, potassium channel with similar properties to those reported for transient expression in *Xenopus* oocytes.

3 Perhexiline caused voltage- and frequency-dependent block of HERG (IC_{50} 7.8 μM).

4 The rate of inactivation was increased and there was a 10 mV hyperpolarizing shift in the voltage-dependence of steady-state inactivation, suggestive of binding to the inactivated state.

5 In conclusion, perhexiline potently inhibits transfected HERG channels and this is the probable mechanism for QT prolongation and *torsades de pointes*. Channel blockade shows greatest affinity for the inactivated state.

Keywords: Perhexiline; human ether-a-go-go-related gene (HERG); Chinese hamster ovary (CHO-K1) cell; cardiac arrhythmia; *torsades de pointes*

Abbreviations: CHO-K1, Chinese hamster ovary; CPT-1, carnitine palmitoyl transferase-1; E_{rev}, reversal potential; HEPES, *N*-2-hydroxylethylpiperazine-N^1-2-ethanesulphonic acid; HERG, human ether-a-go-go-related gene; IC_{50}, drug concentration producing 50% channel blockade; I_K, delayed rectifier potassium channel; I_{Kr}, rapidly activating component of delayed rectifier potassium channel; I_{Ks}, slowly activating component of delayed rectifier potassium channel; I_{Kur}, ultra-rapidly activating potassium channel; $V_{1/2}$, voltage of half maximal activation or inactivation

Introduction

Repolarization of cardiac ventricular myocytes is due mainly to outward potassium currents, the most important of which is the delayed rectifier potassium channel, (I_K), which has both rapidly and slowly activating components (I_{Kr} and I_{Ks}) (Sanguinetti & Jurkiewicz, 1990). Drugs which cause QT prolongation and *torsades de pointes* commonly act by inhibiting I_{Kr}, which is encoded by the human ether-a-go-go-related gene (HERG) (Curran *et al*, 1995; Sanguinetti *et al*., 1995). Class III antiarrhythmic drugs, such as dofetilide (IC_{50} = 3.9 – 320 nM) are well recognized, potent inhibitors of I_{Kr} and HERG-encoded channels (Carmeliet, 1992; Ficker *et al*., 1998; Snyders and Chaudhary, 1996). Recently, several non-cardiac drugs, such as terfenadine (K_D 350 nM, Roy *et al*., 1996), haloperidol (IC_{50} 1 μM, Seussbrich *et al*., 1997), and cisapride (IC_{50} 6.5 nM, Mohammad *et al*., 1997 and 44.5 nM, Rampe *et al*., 1997) have also been recognized as potent HERG channel inhibitors.

Perhexiline has been used clinically as an anti-anginal agent for over 25 years (Cole *et al*., 1990; Horowitz *et al*., 1995). More recently, it has also been reported to improve symptomatic status in elderly patients with aortic stenosis (Unger *et al*., 1997). Perhexiline had antiarrhythmic properties, including reduction of ventricular extrasystoles and atrial arrhythmias (Sukerman, 1973; Drake *et al*., 1973; Pickering & Goulding, 1978). It increases total action potential duration *via* prolongation of phase 3 repolarization and increases the ventricular effective refractory period in the mammalian heart (Ten Eick & Singer, 1973). In addition, perhexiline increases QT duration, without affecting PR or QRS intervals, on the 12-lead electrocardiogram (Drake *et al*., 1973). There has been one case report of *torsades de pointes* in association with perhexiline therapy in a patient admitted with unstable angina (Kerr & Ingham, 1990).

Perhexiline reduces anginal symptoms *via* inhibition of cardiac and hepatic carnitine palmitoyl transferase-1 (CPT-1), thus decreasing fatty acid utilization and increasing lactate use, which reduces myocardial oxygen demand (Kennedy *et al*., 1996). Decreased long chain fatty acid production may produce an anti-arrhythmic effect in the presence of ischaemia, since other inhibitors of CPT-1 delay the cellular uncoupling effects of ischaemia in cardiac tissue (Yamada *et al*., 1994). Blockade of voltage-dependent Ca^{2+} channels (Barry *et al*., 1985) and Na^+ channels (Grima *et al*., 1988) may also confer anti-arrhythmic properties. Perhexiline causes potent, voltage-dependent blockade of the Kv1.5 potassium channel in human embryonic kidney cells (IC_{50} 1.5 μM) and also inhibits the ultra-rapidly activating K^+ channel (I_{Kur}), encoded by Kv 1.5, in human atrial myocytes (Rampe *et al*., 1995). However, this channel is far more abundant in human atrial than ventricular muscle and its blockade by perhexiline is unlikely to explain QT prolongation and *torsades de pointes*.

We used Chinese hamster ovary (CHO-K1) cells stably transfected with HERG to express a delayed rectifier K^+ channel with properties very similar to I_{Kr} and studied the effects of perhexiline on current amplitude and kinetics.

*Author for correspondence at Department of Medicine, St Vincent's Hospital, Darlinghurst, NSW 2010, Australia;
E-mail: b.walker@garvan.unsw.edu.au

Methods

Molecular biology

The CHO-K1 cells (American Type Culture Collection, Bethesda, MD, U.S.A.) used in the following experiments were maintained in Dulbecco's modified Eagle's medium-F12 (DMEM-F12, Gibco, BRL, Gaithersburg, MD, U.S.A.), supplemented with 5% foetal calf serum. Eukaryotic expression of HERG was performed by directionally cloning the coding region of the HERG gene (gift from Dr G. Robertson, Department of Physiology, University of Wisconsin Medical School, Madison, WI, U.S.A.) into the expression vector pRc/CMV (Invitrogen, San Diego, CA, U.S.A.), which also carries the G418 resistance gene. This construct was then transfected into CHO-K1 cells. Cell monolayers in 35 mm^2 dishes were transfected using 9 μl Lipofectamine Reagent (Gibco, BRL) and 1 μg DNA. Stably transfected cells were then selected with 1000 $\mu g\ ml^{-1}$ G418 (Boehringer, Mannheim). These were subcloned to isolate individual cell clones which expressed substantial HERG-related K^+ current. Individual subclones were maintained long-term in tissue culture and used for the patch clamping experiments to be described below.

Electrophysiology

Currents were recorded at room temperature (20–22°C), using the whole-cell patch-clamp technique. CHO-K1 cells plated on coverslips were placed at the bottom of a 2 ml perfusion chamber mounted on the stage of an inverted phase contrast microscope (Nikon Diaphot, Nikon Corporation, Tokyo, Japan). Electrodes were positioned using a micromanipulator (Narishige WB 90, Tokyo, Japan). A silver/silver-chloride reference electrode was either placed directly in the perfusion chamber or in a separate chamber connected by a salt bridge. Membrane potentials were adjusted by −15 mV to correct for the junction potential between high K^+ pipette and external bath solution (calculated using commercial software, JpCalc, Barry, 1994). Cells were patched using micropipettes fabricated from thin-walled borosilicate glass (Vitrex Microhematocrit Tubes, Modulohm 1/S, Denmark) with a vertical pipette puller (Model 720, David Kopf Instruments, CA, U.S.A.). Tip diameters varied between 0.9 and 1.5 μm (pipette resistance = 5.9 ± 2.9 MΩ, $n = 24$). Currents were amplified and filtered at 2 kHz with a 4 pole Bessel filter (−3 dB point) using an Axopatch 1D amplifier (Axon Instruments, Foster City, CA, U.S.A.). Stimulation protocols and data acquisition were carried out using a microcomputer (IBM Pentium), running commercial software and hardware (pClamp 6.0/Digidata 1200, Axon Instruments Inc. and Scientific Solutions Inc.).

Whole-cell capacitance was determined from capacitative transient decay in current recordings following voltage steps of ±10 mV from the holding potential. The median CHO-K1 cell capacitance was 47.7 pF (range 11.2–209 pF). At least 80% series resistance compensation was achieved in all reported experiments (series resistance 13.3 ± 6.4 MΩ before compensation). Leak subtraction was performed in some experiments by applying three hyperpolarizing pre-pulses before the test pulses (P/3 subtraction protocol).

Solutions and drugs

The intracellular pipette solution contained (mM): K gluconate 120, KCl 20, MgATP 1.5, EGTA 5, *N*-2-hydroxylethylpiperazine-*N*[1]-2-ethanesulphonic acid (HEPES) 10, adjusted to pH 7.3. The superfusion solution contained (mM): NaCl 130, KCl 4.8, $MgCl_2$ 1.2, NaH_2PO_4 1.2, HEPES 10, glucose 12.5, $CaCl_2$ 1.0, adjusted to a pH of 7.4. E-4031 (Eisai Corporation, Japan) was made as stock solution dissolved in HEPES-buffered saline solution and stored at −4°C. Perhexiline maleate was purchased from Sigma chemicals (St Louis, MO, U.S.A.) and prepared as stock solution in absolute ethanol (maximum final concentration = 0.1% vol vol^{-1}). In preliminary experiments, we confirmed that ethanol at 0.1% vol vol^{-1} had no effect on the parameters under study.

Statistics

Current analysis was performed using the Clampfit module of the pClamp software. Data are expressed as mean ± s.e. for n experiments. Statistical analyses were performed using Prism 2.0 (Graphpad Software, San Diego, CA, U.S.A.) and Microcal Origin 4.0 (Microcal Software, Northampton, MA, U.S.A.). Unpaired t-tests were used for comparisons of two groups and repeated measures ANOVA with *post-hoc* comparison of means using Dunnett's test for multiple group comparisons. A P value < 0.05 was considered significant. The amplitude of the activating current was calculated as the difference between the initial current recorded just after the step depolarization and the maximum reached at the end of the step. Similarly, the amplitude of the tail current was recorded as the difference between the peak and steady state current after repolarization to −55 mV. The voltage-dependence of current activation was determined by fitting the values of the normalized tail currents to a Boltzmann function:

$$I = 1/(1 + \exp[(V_{1/2} - V_t)/k]),$$

where I represents the relative tail current, $V_{1/2}$, the voltage at which the current was half activated, V_t, the test potential and k, the slope factor. The relationship between drug concentration and current blockade was determined by fitting values to a Hill equation after normalization of post-drug current to control current:

$$I = 1/[+(IC_{50}/D^n],$$

where I represents the relative tail current, IC_{50} the concentration required for 50% channel blockade, D the drug concentration and n the Hill coefficient.

Results

Characteristics of HERG current

Activating currents Non-transfected CHO-K1 cells had a resting membrane potential of −31 ± 2.6 mV ($n = 30$) and insignificant endogenous currents which were disregarded in our analysis (Figure 1a). Whole-cell voltage clamp recordings of HERG-transfected cells revealed currents ('HERG currents') with biophysical properties similar to those reported by previous investigators. Current-voltage relations and activation kinetics were determined using step depolarizations to potentials between −35 and +25 mV from a holding potential of −55 mV (Figure 1b). Activating current amplitude increased with voltage to a maximum at −5 mV (Figure 1c), then declined at more positive potentials due to strong inward rectification. Tail current amplitude increased to a plateau at +5 mV (Figure 1d) and displayed a sigmoidal voltage-dependence which was well fit by a Boltzmann function, yielding a voltage of half maximal activation ($V_{1/2}$) of −15.8 ± 1.0 mV and a slope factor of 6.9 ± 0.9 ($n = 9$).

Inward rectification and deactivation were further studied with a second protocol in which HERG was fully activated with a 500 ms depolarizing pulse to +25 mV, after which, tail currents were elicited by stepping back to potentials between −115 and −15 mV (Figure 2a). The slope of the linear fit of current amplitudes to voltage between −115 and −75 mV gave an estimate for channel conductance of 0.44 pS/pF (Figure 2b). The calculated reversal potential (E_{rev}) was

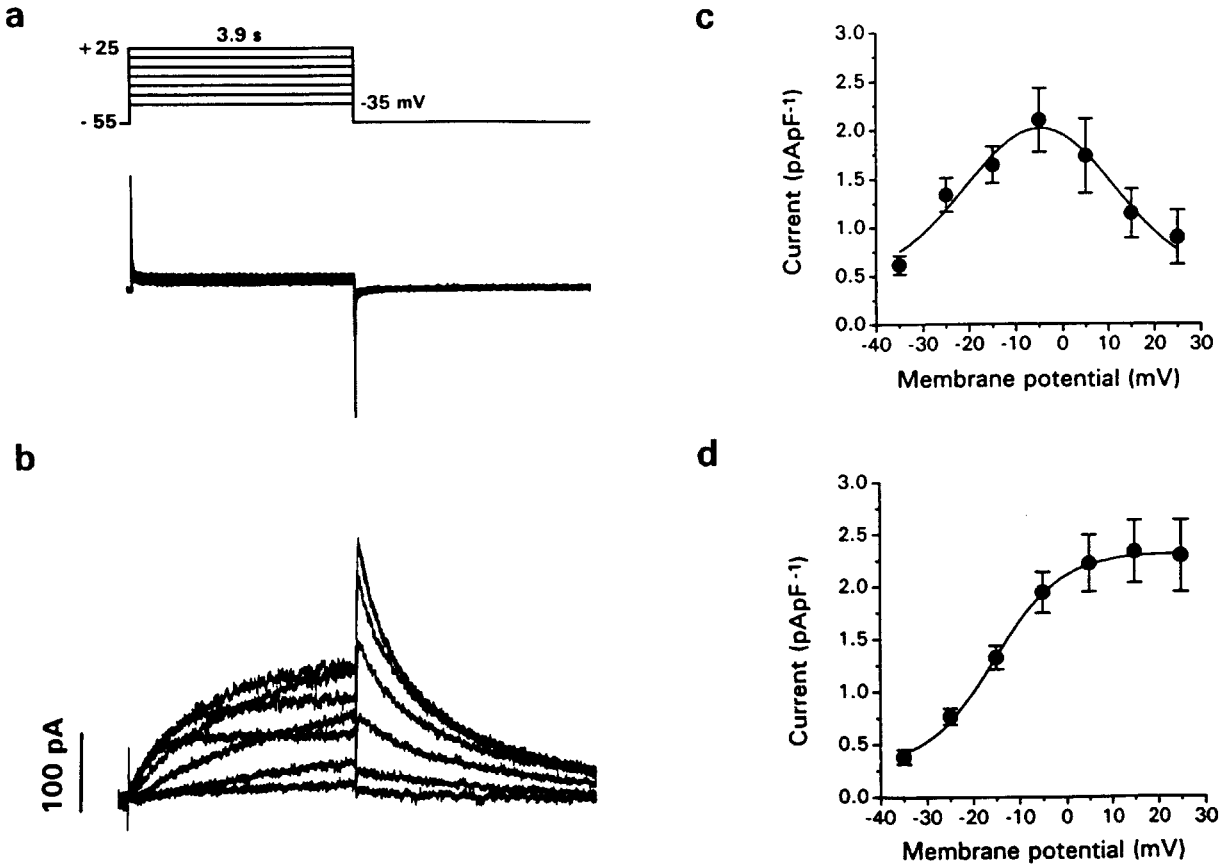

Figure 1 Biophysical properties of HERG stably expressed in CHO-K1 cells. Currents in (a) non-transfected and (b) transfected CHO-K1 cells were elicited by 3.9 s depolarizing steps to potentials between −35 and +25 mV from a holding potential of −55 mV. Both current traces were plotted using the same scale. (c) Current-voltage relation for activating currents. Note that current amplitude increases with voltage to a maximum at −5 mV then inwardly rectifies at positive potentials. Data points were fitted by a Gaussian function. (d) Tail currents from (b) were normalized and fitted with a Boltzmann function $V_{1/2}$ = −15.8 ± 1.0 mV; k = 6.9 ± 0.9, n = 9).

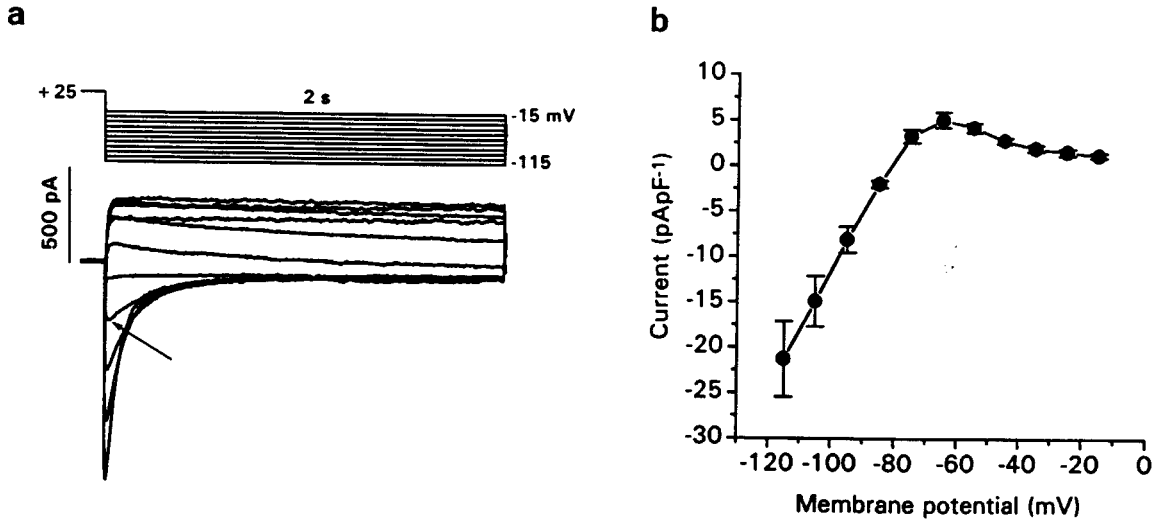

Figure 2 Fully activated HERG current. (a) Currents evoked by 500 ms depolarizing pulse to +25 mV, followed by a 2 s step to potentials between −115 and −15 mV. The arrow indicates the initial 'hook' in the tail current which was well fitted by a single exponential function allowing an estimate of the time constant of recovery from inactivation at each voltage step. (b) Fully activated current-voltage relationship demonstrates a linear (ohmic) relation for inward current, reversal potential of −81.9 mV and inward rectification at potentials above −65 mV.

−81.9 mV (c.f. predicted E_{rev} −86.8 mV at external $[K^+]$ 4.8 mM).

Channel kinetics

Activation The time course of current activation was assessed by fitting each activating current in Figure 1b to a single exponential function (for example: $\tau = 641 \pm 72$ ms at +5 mV, $n = 9$). The rate of activation was voltage dependent, being most rapid at positive potentials (Figure 3a).

Deactivation The time course of deactivation was established by fitting double exponential functions to the tail currents in Figures 1b and 2a (for example: $\tau_{fast} = 603 \pm 51$ ms, $\tau_{slow} = 3992 \pm 392$ ms at −55 mV, following a voltage step to +25 mV, $n = 23$). Deactivation also exhibited voltage-dependent kinetics, with τ_{fast} increasing as voltage became more positive (Figure 3a).

Inactivation A 'dual-pulse' protocol (Smith *et al*., 1996; Spector *et al*., 1996) was used to assess rapid inactivation. Currents were recorded after a 500 ms depolarization to +25 mV from a holding potential of −55 mV, followed by a 20 ms hyperpolarizing step to −125 mV to relieve rapid inactivation, then a second depolarization to potentials between −35 and +25 mV (Figure 3b). The resulting current-voltage relation was linear to a potential of +15 mV (Figure 3c). This confirms that the mechanism for the apparent inward rectification of the HERG current is rapid, voltage-dependent inactivation, as previously shown in other expression systems (Smith *et al*., 1996; Spector *et al*., 1996). The time course for the onset of rapid inactivation was determined by fitting a single exponential function to the tail current elicited after the second depolarizing step. This yielded a time constant of 8.4 ± 1.3 ms at +25 mV ($n = 9$). Recovery from inactivation was determined by fitting a single exponential function to the initial 'hook' preceding slower deactivation of the tail currents in Figure 1c. Both the onset of and recovery from fast inactivation were voltage-dependent and described by a bell-shaped curve, peaking between −25 and −5 mV (Figure 3d).

HERG current inhibition by E-4031

One of the features which has identified HERG as the gene encoding human I_{Kr} is the sensitivity of the channel to class III antiarrhythmic drugs (Kiehn *et al*., 1996; Snyders and Chaudhary 1996; Spector *et al*., 1996; Trudeau *et al*., 1995; Zhou *et al*., 1997). Figure 4a demonstrates the effects of E-4031 300 nM on HERG activating and tail currents. Detailed dose-

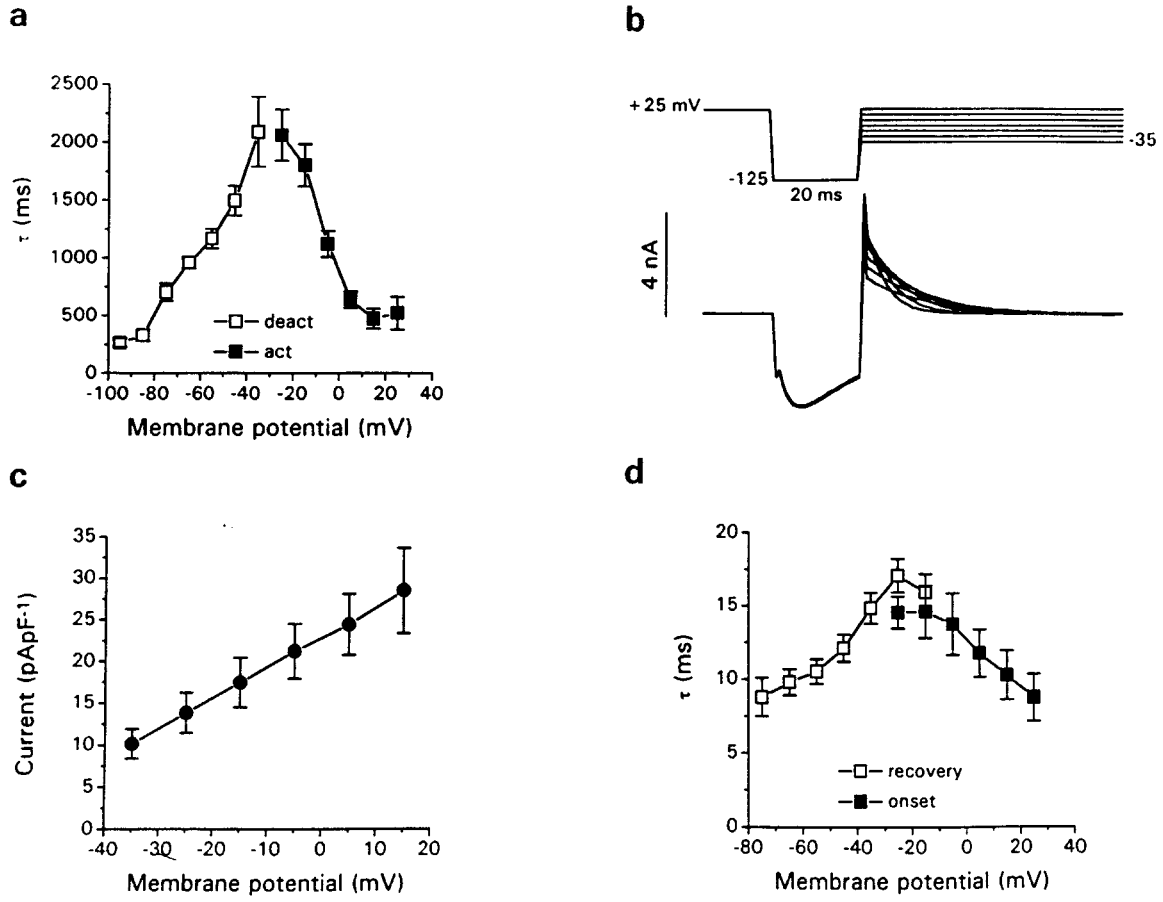

Figure 3 HERG channel kinetics. (a) Activation time constants were derived from currents in Figure 1b fitted with a single exponential function, whereas the time course of deactivation was described by a double exponential function (only τ_{fast} of deactivation plotted). (b) Currents recorded after removal of rapid inactivation. A 500 ms step to +25 mV from a holding potential of −55 mV, was followed by a 20 ms hyperpolarizing interpulse to −125 mV, then a second 500 ms depolarizing step to between −35 and +25 mV elicited large tail currents. Only the currents evoked by the second depolarization are shown. (c) Tail currents in (b) are described by a linear current-voltage relation following removal of inactivation. (d) Time constants for onset of inactivation and recovery from inactivation were derived from tail currents in (b) and the 'hooks' of the currents in Figure 2a, respectively.

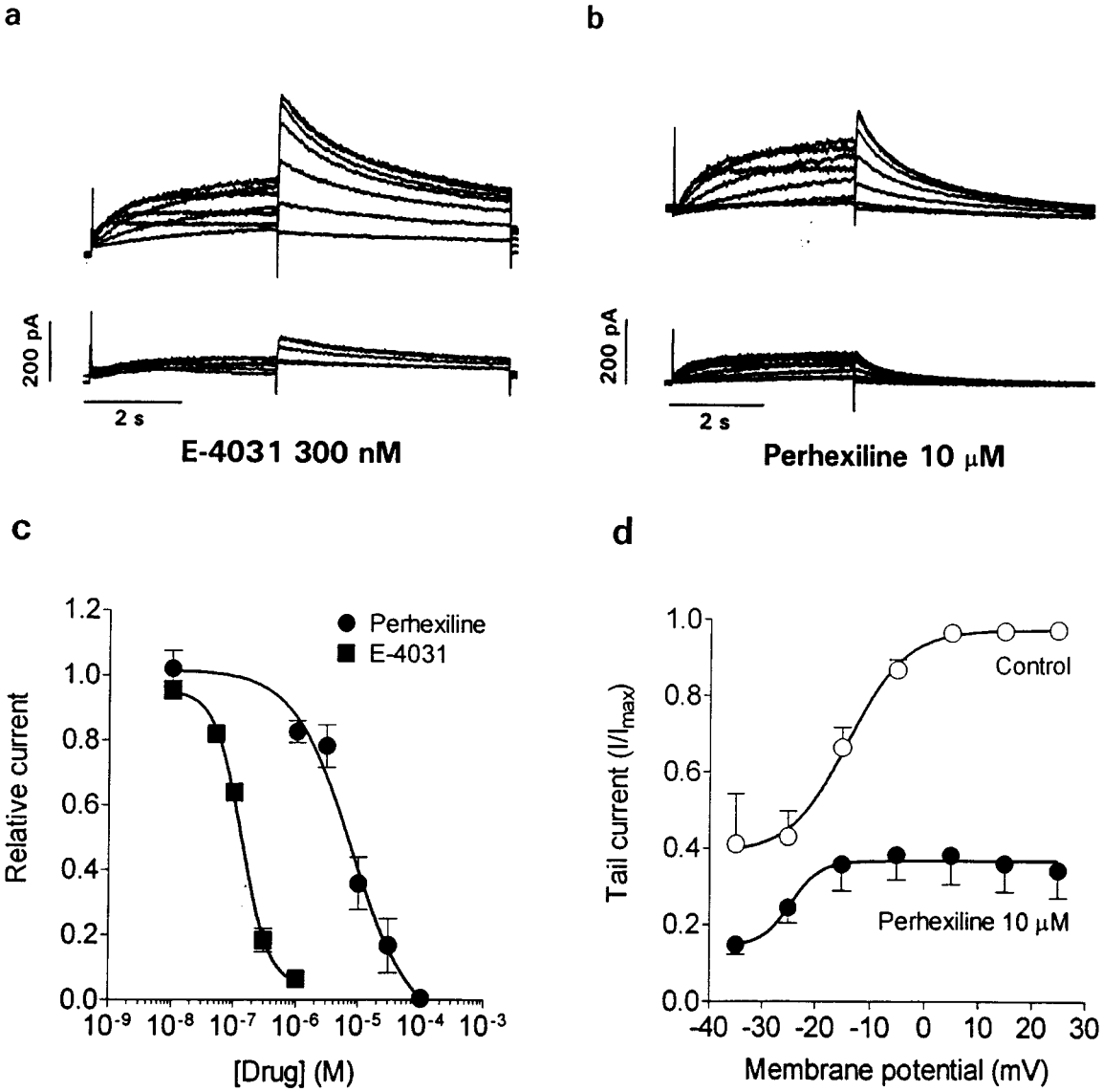

Figure 4 HERG current inhibition by E-4031 and perhexiline. Using the protocol described in Figure 1b, currents were elicited before and after bath superfusion with (a) E-4031 300 nM and (b) perhexiline 10 μM. (c) Relative tail currents ($I_{drug}/I_{control}$) at +25 mV were fitted with a Hill equation and yielded an IC_{50} of 134 nM for E-4031 and 7.8 μM for perhexiline (Hill slope: −2.0 and −2.2, respectively). (d) Tail currents before and after bath exchange with perhexiline 10 μM were normalized to the maximum control current, then fitted to a Boltzmann function ($V_{1/2}$ shifted from −16.1 to −24.5 mV after application of perhexiline).

response studies of the blockade of HERG tail current (Figure 4c) following a step to +25 mV yielded an IC_{50} for E-4031 of 134 nM (95%CI 113–160 nM, $n=5$).

Effects of perhexiline

HERG current inhibition Perhexiline (0.01–100 μM) inhibited activating and tail currents with equal potency (Figure 4b). The observed IC_{50} was 7.8 μM (CI 1.8–35.0) for inhibition of tail currents following a depolarization to +25 mV (Figure 4c). Perhexiline 10 μM shifted the voltage of half maximal activation ($V_{1/2}$) from -16.1 ± 0.8 mV in controls to -24.5 ± 1.2 mV ($P<0.01$, $n=7$). HERG tail current inhibition was weakly voltage-dependent, increasing from $42.6\pm6.9\%$ at −35 mV to $64.2\pm8.1\%$ at +25 mV ($P=0.07$, $n=6$, Figure 4d). Drug washout was relatively fast with tail currents recovering to $88\pm3\%$ of control values 5 min after removal of perhexiline from the superfusate ($n=7$). Recovery from channel blockade was independent of the number of pulses applied during the washout period.

Effect of pulse duration of HERG inhibition The effect of pulse duration on channel blockade by perhexiline 10 μM was studied in two ways (Figure 5). In the first of these, single voltage steps from a holding potential of −55 mV to +25 mV and then back to −55 mV were applied at 10 s intervals. The duration of each of these steps was progressively increased from 0.12–13 s (Figure 5a). It can be seen in Figure 5b that most (~75%) of the blocking effect of perhexiline was already present after the first of these pulses (37% reduction from control), and that no significant increment in blockade occurred with increasing pulse duration ($n=7$).

A similar finding was seen with the second protocol (Figure 5c), in which we observed development of blockade during a single prolonged pulse to +10 mV (preceded by a step to +60 mV to produce activation of all channels; (Mohammad *et al.*, 1997). Once again, virtually all of the final effect of perhexiline was already present on first stepping to +10 mV. Furthermore, we varied the duration of the drug 'wash-in' while cells were held at −80 mV, than assessed the degree of current inhibition with the first depolarizing step. Current

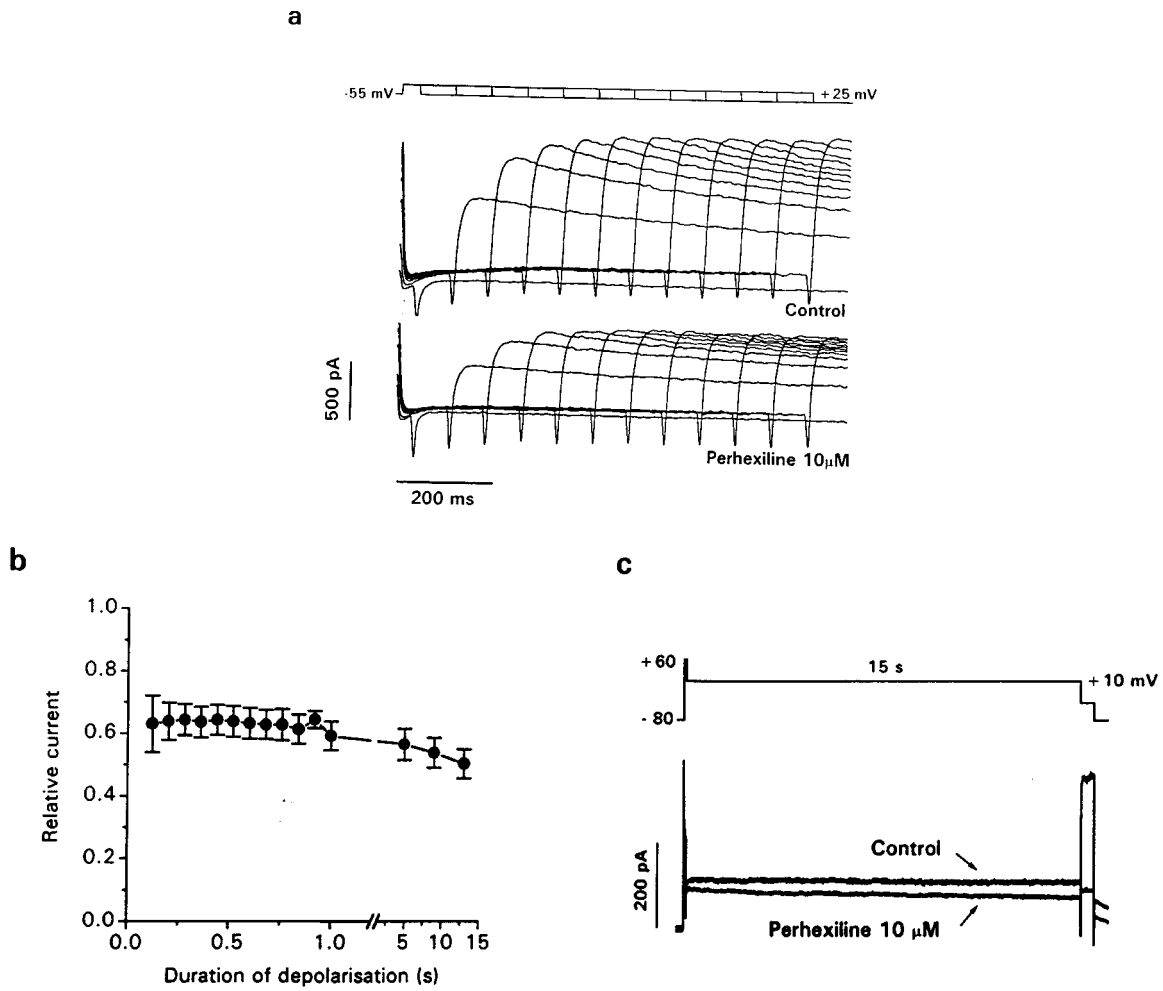

Figure 5 Effect of pulse duration on block by perhexiline 10 μM. (a) Representative current trace produced by voltage steps to +25 mV of variable duration (0.12–13 s) applied at 10 s intervals. (b) Tail current after each step was expressed as relative current and plotted as a function of the duration of the depolarizing step. Channel block was 37% after a 120 ms voltage step, and did not significantly increase with longer depolarizations. (b) Blockade during a prolonged depolarization. Representative current traces (control and after perhexiline 10 μM) produced by a 100 ms depolarizing step to +60 mV, after which cells were clamped at +10 mV for 15 s, then returned to −60 mV.

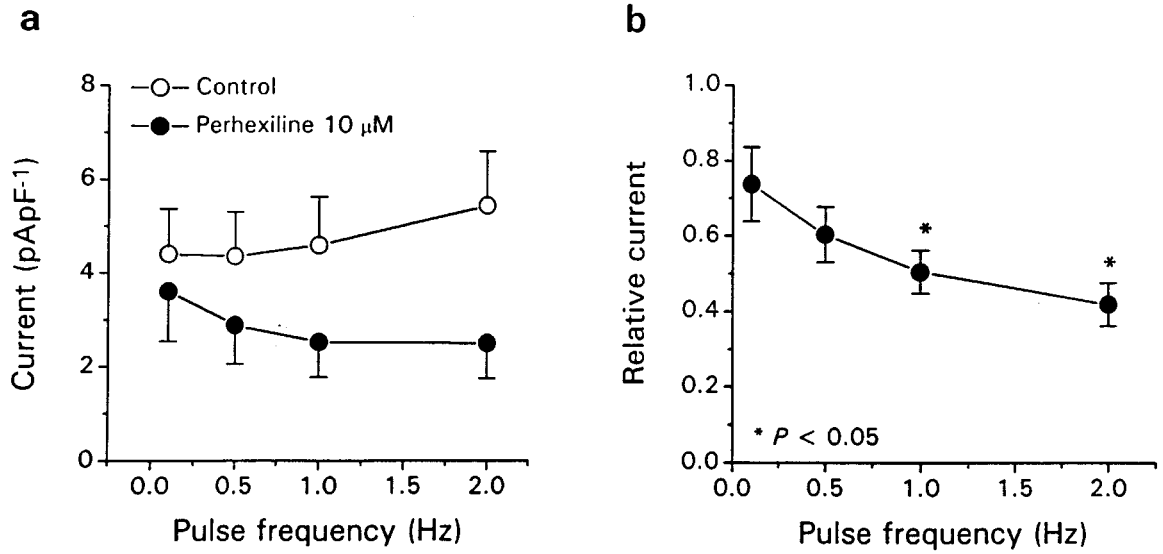

Figure 6 Frequency-dependence of channel blockade by perhexiline 10 μM. Following a conditioning train of 200 ms depolarizations to +15 mV for 1 min at frequencies between 0.1–2 Hz, tail currents were recorded after a single 500 ms voltage step to +15 mV. (a) Tail current amplitudes plotted as a function of pulse frequency. There was a trend towards an increase in control current amplitude as stimulation frequency increased. (b) Data from (a) expressed as relative current. Channel blockade significantly increased with pulse frequency (*$P<0.05$ for data points at 1.0 and 2.0 Hz relative to 0.1 Hz).

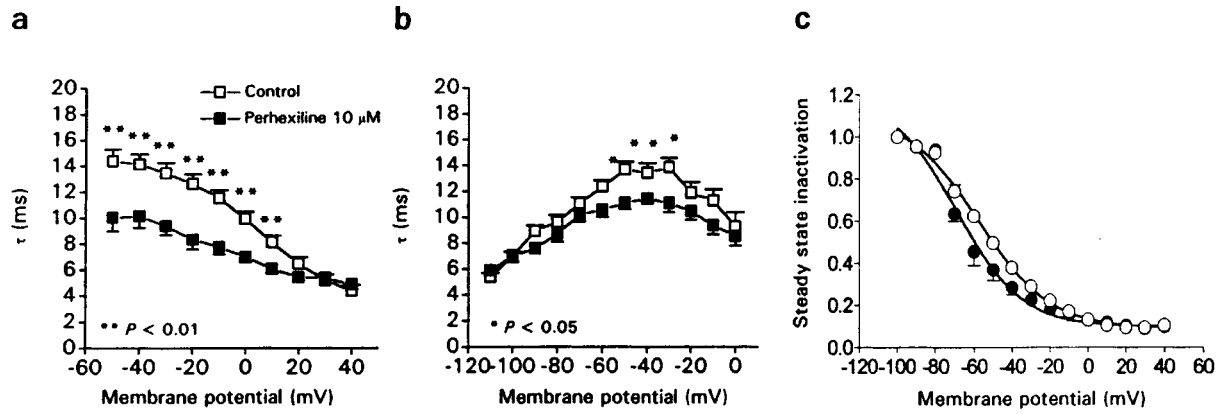

Figure 7 Modulation of channel gating by perhexiline. Time constants obtained using similar methods described in Figure 3 before and after perhexiline 10 μM. (a) Inactivation time constants are significantly reduced at most membrane potentials. (b) Recovery from inactivation is accelerated only at potentials between -60 and -30 mV, with a similar trend at positive potentials. (c) Steady state inactivation in controls and after superfusion with perhexiline 10 μM obtained from a 'dual pulse' protocol described in the text. Data points were fit independently to Boltzmann functions, demonstrating a 10 mV hyperpolarizing shift in steady state inactivation ($V_{1/2}$: -57.4 mV versus -68.6 mV after perhexiline).

inhibition was $27\pm9\%$ immediately after bath exchange, compared with $32\pm5\%$ following a 4 min wash-in period (P=ns, $n=7$).

Frequency-dependence of HERG blockade by perhexiline A conditioning train of 200 ms depolarizations from -55 mV to $+15$ mV was applied for 1 min at a frequency of 0.1, 0.5, 1 or 2 Hz. Immediately after each train, tail current amplitudes were measured following a single voltage step to $+15$ mV (Figure 6). While a trend towards increase in tail current in controls was noted as stimulation frequency increased (17% increase following 2 Hz stimulation), this did not reach statistical significance ($n=14$). Tail current inhibition by perhexiline 10 μM increased from $26.4\pm9.9\%$ after stimulation at 0.1 Hz to $58.3\pm5.6\%$ following a conditioning train at 2 Hz ($P<0.05$, $n=5$, Figure 6b).

Modulation of HERG gating properties by perhexiline The time course of HERG channel activation and deactivation was not significantly changed by perhexiline 10 μM (data not shown). However, inactivation was significantly accelerated at most potentials (Figure 7a). Following a voltage step to -5 mV, the time constant of inactivation decreased from 10.5 ± 0.5 ms in controls to 7.4 ± 0.1 ms after perhexiline ($P<0.01$, $n=4-6$). Recovery from inactivation was also accelerated by perhexiline 10 μM, although this was only significant from membrane potentials between -60 and -30 mV (Figure 7b). Steady state inactivation was obtained from a 'dual pulse' protocol described by Wang *et al.* (1997) and studied in the presence of perhexiline 10 μM (Figure 7c). A 500 ms step to $+30$ mV was followed by a 40 ms interpulse to -80 mV, then a series of depolarizing steps to between -100 and $+40$ mV. The ratio of currents measured 100 ms after the onset of the second depolarizing pulse to the instantaneous currents at the same potential was plotted relative to the degree of inactivation at -80 mV. For steps between -80 and -100 mV, the increase in current relative to that occurring at -100 mV was used to calculate steady state inactivation. Perhexiline caused a modest hyperpolarizing shift in the voltage-dependence of steady-state inactivation ($V_{1/2}$ -57.4 ± 1.8 mV in controls and -68.6 ± 4.4 mV after perhexiline, $P<0.05$, $n=6-11$).

Discussion

Characterization of HERG current

This study demonstrates that HERG, stably expressed in CHO-K1 cells produces a delayed rectifier channel with similar biophysical properties to those reported in *Xenopus* oocytes transiently transfected with HERG (Sanguinetti *et al.*, 1995; Trudeau *et al.*, 1995) or in human embryonic kidney cells (Snyders & Chaudhary, 1996, transient transfection; Zhou *et al.*, 1997, stable chronic transfection). HERG has been transiently transfected into CHO-K1 cells previously (McDonald *et al.*, 1997), but to our knowledge a stable transfection into CHO-K1 cells has not been described.

The voltage-dependence of channel activation closely approximates that described by Snyders and Chaudhary (1996) and Sanguinetti *et al.* (1995), but is more negative than that obtained by McDonald *et al.* (1997). As with all other reported expression systems for HERG, the kinetics of channel activation and deactivation are significantly slower than those described for I_{Kr} in mammalian myocytes (Shibisaki, 1987; Sanguinetti & Jurkiewicz, 1990; Yang *et al.*, 1994). Application of the 'dual pulse' protocol confirmed that rapid inactivation is the mechanism for the inward rectification of HERG channels (Smith *et al.*, 1996; Spector *et al.*, 1996). A use-dependent increase in I_{Kr} tail current amplitude (Figure 6a) has been described by Carmeliet (1993) when cells were pulsed at 1.33 Hz. Although not previously described for HERG channels, this is probably due to accumulation of channels in the open state, since deactivation is incomplete at this frequency.

HERG channel blockade by E-4031 occurred with potency similar to that reported by Trudeau *et al.* (1995) (IC_{50} 588 nM).

Perhexiline

In our studies, perhexiline inhibited HERG channels at clinically relevant concentrations. Therapeutic plasma concentrations usually vary between 0.5–2 μM, but levels of 7–8 μM have been described in patients treated with high doses (Horowitz *et al.*, 1986). Perhexiline undergoes phase 1 oxidative metabolism by P450 2D6 and has readily saturable

hepatic metabolism within usual clinical dose ranges (Horowitz *et al*., 1995). Eight to ten per cent of Caucasians are 'poor metabolizers' of perhexiline due to a genetic polymorphism of the major metabolic pathway by cytochrome P450 2D6 (Peck *et al*., 1993; Horowitz *et al*., 1995). As a result, these patients are especially prone to having high plasma concentrations with consequent susceptibility to adverse effects.

Perhexiline caused a hyperpolarizing shift in the voltage-dependence of HERG channel activation. Current inhibition was greater at more positive potentials, at which most channels would be in the inactivated state. Furthermore, channel blockade was frequency-dependent. These observations suggest that perhexiline preferentially binds to either open or inactivated states or both. The lack of significant incremental blockade during prolonged depolarizations (Figure 5) suggests that any open or inactivated state binding either occurs very rapidly or that the closed state is also bound. Toyama *et al*. (1997) found that I_K tail blockade by E-4031 in rabbit ventricular myocytes was similarly unaffected by pulse duration, and drew similar conclusions to ours.

Rampe *et al*. (1995) provide evidence for open channel blockade by perhexiline in their studies of Kv1.5 expressed in human embryonic kidney cells by demonstrating accelerated current decay during step depolarizations as well as slower deactivation. They suggested that perhexiline may access an intracellular binding site in Kv1.5 on the basis of mildly increased block observed at positive potentials, caused by the positively charged fraction of the drug, approximately 5% at physiological pH (pKa = 6.1). The Kv1.5 current is a rapidly activating and relatively slowly inactivating delayed rectifier current and this differs significantly from the HERG channel. In our experiments, perhexiline did not modify the time course of channel activation. If present, a tail current 'crossover', due to transient channel unblocking during repolarization (Snyders *et al*., 1992), provides additive evidence for open channel block. This was not seen in our experiments and the time course of deactivation remained unchanged in the presence of perhexiline.

The time course and use-dependence of drug washout may provide further evidence regarding the state dependence of channel blockade. Use-dependent unbinding during washout may indicate trapping of the drug in a blocked state due to closure of the activation gate (Carmeliet, 1993) and is consistent with open channel blockade (Snyders *et al*., 1996). In our experiments drug 'washout' was nearly complete within 5 min and was not use dependent suggesting that significant drug trapping did not occur.

Perhexiline markedly accelerated inactivation at most potentials, consistent with the observed 10 mV hyperpolarizing shift in the voltage-dependence of steady state inactivation, which implies a decrease in channel availability (Smith *et al*., 1996). Perhexiline also modestly increased the rate of recovery from inactivation. These data all suggest that the drug binds to the inactivated channel state, although open state binding has not been fully excluded.

Previous studies have shown that HERG channel inactivation is critically dependent on several amino acids in the outer pore region, including G628 and G631 (Smith *et al*., 1996; Schonherr & Heinemann, 1996; Zou *et al*., 1998). Similarly, a report by Ficker *et al*. (1998) found that mutation of a serine residue on the cytoplasmic side of the pore (S620T) is associated with loss of C-type inactivation and removal of high affinity block by dofetilide. Recently, Nakajima *et al*. (1998) demonstrated that the co-expression of two HERG mutations (A614V and V630L) in the pore region with wild-type HERG resulted in a similar hyperpolarizing shift in the voltage dependence of steady state inactivation to that evoked by perhexiline. We therefore postulate that perhexiline may bind to the channel in the pore region and that binding is dependent on one or more of the above sites.

In conclusion, we have demonstrated that the biophysical properties of HERG channels in a stably transfected, mammalian cell line do not substantially differ from the channel when transiently expressed in other cells. Inhibition of HERG channels by perhexiline occurs at clinically relevant concentrations and is the probable cellular mechanism for QT prolongation and *torsades de pointes*. Perhexiline binds with greatest affinity to the inactivated channel state.

Dr B.D. Walker and Dr S.M. Valenzuela were equal contributors to this paper. This work was supported by research grants from the National Health and Medical Research Council of Australia, National Heart Foundation of Australia, St Vincent's Clinic and The Clive and Vera Ramaciotti Foundation.

References

BARRY, P.H. (1994). JPCalc, a software package for calculating liquid junction potential corrections in patch-clamp, intracellular, epithelial and bilayer measurements and for correcting junction potential measurements. *J. Neurosci. Meth.,* **51,** 107–116.

BARRY, W.H., HOROWITZ, J.D. & SMITH, T.W. (1985). Comparison of negative inotropic potency reversibility and effects on calcium influx of six calcium channel antagonists in cultured myocardial cells. *Br. J. Pharmacol.,* **85,** 51–59.

CARMELIET, E. (1992). Voltage- and time-dependent block of the delayed K+ current in cardiac myocytes by dofetilide. *J. Pharm. Exp. Ther.,* **262,** 809–817.

CARMELIET, E. (1993). Use-dependent block and use-dependent unblock of the delayed rectifier K+ current by almokalant in rabbit ventricular myocytes. *Circ. Res.,* **73,** 857–868.

COLE, P.L., BEAMER, A.D., MCGOWAN, N., CANTILLON, C.O., BENFELL, K., KELLY, R.A., HARTLEY, L.H., SMITH, T.W. & ANTMAN, E.M. (1990). Efficacy and safety of perhexilene maleate in refractory angina. *Circulation,* **81,** 1260–1270.

CURRAN, M.E., SPLAWSKI, I., TIMOTHY, K.W., VINCENT, G.M., GREEN, E.D. & KEATING, M.T. (1995). A molecular basis for cardiac arrhythmia: HERG mutations cause long QT syndrome. *Cell,* **80,** 795–803.

DRAKE, F.T., HARING, O., SINGER, D.H. & DIRNBERGER, G. (1973). Evaluation of the anti-arrhythmic efficacy of perhexilene maleate in ambulatory patients by Holter monitoring. *Postgraduate Med. J.,* (April Supp) 52–63.

FICKER, E., JAROLIMEK, W., KIEHN, J., BAUMANN, A. & BROWN, A. (1998). Molecular determinants of dofetilide block of HERG K+ channels. *Circ. Res.,* **82,** 386–395.

GRIMA, M., VELLY, J., DECKER, N., MARCINIAK, G. & SCHARWTZ, J. (1988). Inhibitory effects of some cyclohexylaralkylamines related to perhexiline on sodium influx, binding of [^{3}H]batrachotoxin A 20-alpha-benzoate and [^{3}H]nitrendipine and on guinea pig left atria contractions. *Eur. J. Pharmacol.,* **147,** 173–185.

HOROWITZ, J.D., BURTON, I. & WING, L. (1995). Is perhexilene essential for the optimal management of angina pectoris. *Aust. N.Z. J. Med.,* **25,** 111–113.

HOROWITZ, J.D., SIA, S., MACDONALD, P.S., GOBLE, A.J. & LOUIS, W.J. (1986). Perhexilene maleate treatment for severe angina pectoris–correlations with pharmacokinetics. *Int. J. Cardiol.,* **13,** 219–229.

KENNEDY, J.A., UNGER, S. & HOROWITZ, J.D. (1996). Inhibition of carnitine palmitoyltransferase-1 in rat heart and liver by perhexilene and amiodarone. *Biochem. Pharmacol.,* **52,** 273–280.

KERR, G.D. & INGHAM, G. (1990). *Torsade de pointes* associated with perhexilene maleate therapy. *Aust. N.Z. J. Med.,* **20,** 818–819.

KIEHN, J., LACERDA, A.E., WIBLE, B. & BROWN, A.M. (1996). Molecular physiology and pharmacology of HERG, single-channel currents and block by dofetilide. *Circulation,* **94,** 2572–2579.

MCDONALD, T.V., YU, Z., MING, Z., PALMA, E., MEYERS, M.B., WANG, K.W., GOLDSTEIN, S.A.N. & FISHMAN, G.I. (1997). A minK-HERG complex regulates the cardiac potassium current I_{Kr}. *Nature,* **388,** 289–292.

MOHAMMED, S., ZHOU, Z., GONG, Q. & JANUARY, C.T. (1997). Blockage of the HERG human cardiac K+ channel by the gastrointestinal prokinetic agent cisapride. *Am. J. Physiol.,* **273,** H2534–H2538.

NAKAJIMA, T., FURUKAWA, T., TANAKA, T., KATAYAMA, Y., NAGAI, R., NAKAMURA, Y. & HIROAKA, M. (1998). Novel mechanism of HERG current suppression in LQT2. *Circ. Res.,* **83,** 415–422.

PECK, C.C., TEMPLE, R. & COLLINS, J.M. (1993). Understanding consequences of concurrent therapies. *J. Am. Med. Ass.,* **269,** 1550–1552.

PICKERING, T.G. & GOULDING, L. (1978). Suppression of ventricular extrasystoles by perhexiline. *Br. Heart J.,* **40,** 851–855.

RAMPE, D., ROY, M.L., DENNIS, A. & BROWN, A.M. (1997). A mechanism for the proarrhythmic effects of cisapride (Propulsid): high affinity blockade of the human cardiac potassium channel HERG. *FEBS Lett.,* **417,** 28–32.

RAMPE, D., WANG, Z., FERMINI, B., WIBLE, B., DAGE, R.C. & NATTEL, S. (1995). Voltage- and time-dependent block by perhexilene of K+ currents in human atrium and in cells expressing a Kv1.5-type cloned channel. *J. Pharm. Exp. Ther.* **274,** 444–449.

ROY, M.L., DUMAINE, R., BROWN, A.M. (1996). *HERG*, a primary human ventricular target of the nonsedating antihistamine terfenadine. *Circulation,* **94,** 817–823.

SANGUINETTI, M.C., JIANG, C., CURRAN, M.E. & KEATING, M.T. (1995). A mechanistic link between an inherited and an acquired cardiac arrhythmia: HERG encodes the I_{Kr} potassium channel. *Cell,* **81,** 299–307.

SANGUINETTI, M.C. & JURKIEWICZ, N.K. (1990). Two components of cardiac delayed rectifier K+ current. *J. Gen. Physiol.,* **96,** 195–215.

SCHONHERR, R. & HEINEMANN, S.H. (1996). Molecular determinants for activation and inactivation of HERG, a human inward rectifier potassium channel. *J. Physiol.,* **387,** 227–250.

SEUSSBRICH, H., SCHONHERR, R., HEINEMANN, S.H., ATTALI, B., LANG, F. & BUSCH, A.E. (1997). The inhibitory effect of the antipsychotic drug haloperidol on HERG potassium channels expressed in *Xenopus* oocytes. *Br. J. Pharmacol.,* **120,** 968–974.

SHIBASAKI, T. (1987). Conductance and kinetics of delayed rectifier potassium channels in nodal cells of the rabbit heart. *J. Physiol.,* **387,** 227–250.

SMITH, P.L., BAUKROWITZ, T. & YELLEN, G. (1996). The inward rectification mechanism of the HERG cardiac potassium channel. *Nature,* **379,** 833–836.

SNYDERS, D.J. & CHAUDHARY, A. (1996). High affinity open channel block by dofetilide of HERG expressed in a human cell line. *J. Pharm. Exp. Ther.,* **49,** 949–955.

SNYDERS, D.J., KNOTH, K.M., ROBERDS, S.L. & TAMKUN, M.M. (1992). Time-, voltage, and state-dependent block by quinidine of a cloned human cardiac potassium channel. *Mol. Pharmacol.,* **41,** 322–330.

SPECTOR, P.S., CURRAN, M., ZOU, A., KEATING, M.T. & SANGUINETTI, M.C. (1996). Fast inactivation causes rectification of the I_{Kr} channel. *J. Gen. Physiol.,* **107,** 611–619.

SUKERMAN, M. (1973). Clinical evaluation of perhexilene maleate in the treatment of chronic cardiac arrhythmias of patients with coronary heart disease. *Postgraduate Med. J.,* (April Supp) 46–52.

TEN EICK, R.E. & SINGER, D. (1973). Effects of perhexilene on the electrophysiologic activity of mammalian heart. *Postgraduate Med. J.* (April supp) 32–42.

TOYAMA, J., KAMIYA, K., CHENG, J., LEE, J.K., SUZUKI, R. & KODAMA, I. (1997). Vesnarinone prolongs action potential duration without reverse frequency dependence in rabbit ventricular muscle by blocking the delayed rectifier K+ current. *Circulation,* **96,** 3696–3703.

TRUDEAU, M.C., WARMKE, J.W., GANETSKY, B. & ROBERTSON, G.A. (1995). HERT, a human inward rectifier in the voltage-gated potassium channel family. *Science,* **269,** 92–95.

UNGER, S.A., ROBINSON, R.M. & HOROWITZ, J.D. (1997) Perhexilene improves symptomatic status in elderly patients with severe aortic stenosis. *Aust. N.Z. J. Med.,* **27,** 24–28.

WANG, S., LIU, S., MORALES, M.J., STRAUSS, H.C. & RASMUSSON, R.L. (1997). A quantitative analysis of the activation and inactivation kinetics of HERG expressed in *Xenopus* oocytes. *J. Physiol.,* **502,** 45–60.

YAMADA, K.A., MCHOWAT, J., YAN, G-X., DONAHUE, K., PEIRICK, J., KLEBER, A.G. & CORR, P.B. (1994). Cellular uncoupling induced by accumulation of long-chain acylcarnitine during ischaemia. *Circ. Res.,* **74,** 83–95.

YANG, T., WATHEN, M.S., FELIPE, A., TAMKUN, M.M., SNYDERS, D.J. & RODEN, D.M. (1994). K+ currents and K+ channel mRNA in cultured atrial cardiac myocytes. *Circ. Res.,* **75,** 870–878.

ZHOU, Z., GONG, Q., YE, B., FAN, F., MAKIELSKI, J.C., ROBERTSON, G.A. & JANUARY, C.T. (1997). Electrophysiological and pharmacological properties of HERG channels in a stably transfected human cell line (Abstract). *Biophys. J.,* **72,** A225.

ZOU, A., XU, Q.P. & SANGUINETTI, M.C. (1998). A mutation in the pore region of HERG K+ channels expressed in *Xenopus* oocytes reduces rectification by shifting the voltage dependence of inactivation. *J. Physiol.,* **509,** 129–137.

(Received September 23, 1998
Revised January 25, 1999
Accepted January 29, 1999)